Experimental Verification of a Rotor Unbalance Response Based Approach to the Identification of Magnetic Bearing Support Parameters

Long Di[a], Jin Zhou[b], Changli Cheng[b], Zongli Lin[a]

[a] Charles L. Brown Department of Electrical and Computer Engineering, and Rotating Machinery and Control Laboratory (ROMAC), University of Virginia, Charlottesville, VA 22904-4743, USA, {ld4vv, zl5y}@virginia.edu

[b] College of Mechanical and Electrical Engineering, Nanjing University of Aeronautics and Astronautics, nuaazhoujin@gmail.com, 970053197@qq.com

***Abstract*—The support parameters, the stiffness and damping coefficients, of active magnetic bearings (AMBs) have direct influence on the dynamic response and stability of a rotor bearing system. The unbalance response method is a simple but effective way to identify the AMB support parameters. In this paper, we present experimental verification of this identification method. We first briefly introduce the unbalance response method and the error response surface approach to rectifying the identification error induced by the rotor flexibility. The final AMB stiffness and damping coefficients are determined as the sum of the nominal values identified by the unbalance response method and the identification errors derived from the error response surfaces. We will then present the experimental verification of this combined unbalance response and error response surface identification method on a rotor AMB test rig. In order to verify the identification method, the parameters thus identified based on the experimental data are integrated with the rotor finite element model to form the rotor-AMB model. The model unbalance response is obtained through simulation and compared with experimentally measured unbalance response. The close agreement between the model unbalance response and the experimentally measured response demonstrates that the proposed method is effective in identifying the AMB support parameters.**

I. Introduction

Active magnetic bearings (AMBs) find a wide range of applications in energy storage, machine tool operation, artificial heart pumps and hybrid vehicles [1], because of their lubrication free and non-contact operation. The stiffness and damping coefficients of a rotor AMB system have substantial effect on the system dynamic response and stability, and many methods have been reported on their determination. Humphris et al. derived equivalent stiffness and damping coefficients from the AMB system transfer function [2], Yu [3] and Hu et al. [4] analyzed the theoretical AMB static and dynamic characteristics, Wang and Jiang [5] proposed a method to estimate the bearing stiffness using the control current ratio. These methods are based on a simplified model and the support parameters of AMBs are identified only through the theoretical analysis, which leads to inaccurate results. In addition, it is difficult to identify support parameters based on theoretical analysis methods when complex AMB control algorithms are employed.

Compared to the theoretical analysis approach, which requires simplified model of the rotor AMB system, experimental identification approach is an easier but effective way to identify the AMB stiffness and damping coefficients. Wang [6] and Schweitzer et al. [7] confirmed that the AMB stiffness and damping coefficients are closely related to the controller frequency response, with the controller bandwidth having the strongest impact. Yang et al. [8] used the AMB as an exciter for the stiffness identification. Since the excitation force is obtained through the electrical current conversion, magnetic flux leakage causes the actual force to be inconsistent with the theoretical value. Wu [9] and Wang and Gao [10] used the external load method to identify the static stiffness, but they did not consider the dynamic characteristics of magnetic bearings. Zhou and Lin [11] used the hammer impact method to estimate the stiffness and damping of a single degree of freedom (SDOF) AMB system, and then verified the results through the sine sweep frequency response. According to the amplitude-frequency characteristic curve, the estimated system stiffness is close to the value obtained by the hammer impact method, but the study was only limited to an SDOF system. Shen and Yu [12] used the multiple frequency excitation approach, in combination with the least squares method, to identify the AMB support parameters, but a rigid rotor motion equation was used as the rotor model. The drawback for these existing experimental identification approaches is that they mostly do not consider rotor flexibility, which leads to inconsistent results at different rotating speeds.

In summary, there are basically two main approaches to the identification of the AMB support parameters. One is based on the frequency characteristics of the control system, which has been studied through theoretical analysis but lacks experimental verification. The other one is to analyze response to the excitation. The second approach is mostly based on a rigid rotor motion and does not take the rotor flexibility into consideration. Treating the unbalance force an excitation, Zhou et al. [16] developed an unbalance response based method to identify AMB support parameters, which takes the rotor flexibility into consideration during the identification process. The unbalance response based support parameter identification method has already been widely used in mechanical bearings, but few works have been documented for applying this method to AMBs. Because the unbalance force is the simplest form

of external excitation, it does not require additional devices, which makes experimental studies easier to conduct [13]–[15].

In this paper, we present experimental verification of the unbalance response based method that was developed in [16] on a flexible rotor AMB test rig. Two sets of balancing weights are attached to the rotor disks to obtain the unbalanced rotor displacements, from which the nominal stiffness and damping coefficients are derived. We then rectify the identification error caused by the rotor flexibility with an error response surface approach. The final parameters thus identified are integrated with the rotor finite element model to form the rotor-AMB model. The model unbalance response is obtained through simulation and compared with experimentally measured unbalance response. The close agreement between the model unbalance response and the experimentally measured response demonstrates that the proposed method is effective in identifying AMB support parameters.

The remainder of this paper is organized as follows. Section II describes the experimental setup and the unbalance response based method we are to verify. Section III presents the results. Section IV draws a conclusion to the paper.

II. The Identification Method

This section contains three subsections. Subsection II-A describes the flexible rotor AMB test rig where the proposed identification method is applied. The identification results are also verified based on this test rig in Sec. III. Subsection II-B introduces a rigid rotor model based identification method to calculate the nominal values of the AMB stiffness and damping coefficients from the measured unbalance response. Subsection II-C adopts a finite element model of the rotor to construct error response surfaces for rectifying the identification errors induced by the rigid rotor modeling of the flexible rotor.

A. Experimental Setup

Shown in Fig. 1 is the experiment setup that we use to verify the identification method described in Section II. The setup contains a five DOF rotor AMB test rig and two sets of balancing weights that are added to the rotor disks. This test rig was built to simulate an industrial high speed centrifugal gas compressor and two radial AMBs (H and A) are located on the driven (DE) and nondriven end (NDE) of the rotor. The nominal bias current is around 3.8 A so the support AMBs' load capacity is around 1336 N. Each AMB is equipped with four Model 422 PWM amplifiers from Copley Controls and each amplifier can generate up to 10 A current and 3.2 kW peak power output to provide the maximum required force slew rate. The rotor movement is monitored by a 10 channel Kaman eddy current sensor system. For each AMB control axis, there is one pair of sensor probes in a differential arrangement to measure the rotor displacement in the direction of the AMB control quadrants. To avoid damage when the rotor drops, two auxiliary bearings are also mounted in the casing with 10 mils clearance. The steel rotor has a length of 1.23 m and weighs around 44.9 kg. The first rigid body mode is around 2500 RPM (41.67 Hz) and the first bending mode is around 14,800 RPM (246.67 Hz). A 3.7 kW Colombo RS-90/2 high speed motor with variable frequency drive (VFD) is used to move the rotor up to 18,000 RPM.

There are two discs attached to the rotor and they serve as the balance planes. For disc 1, the distance between the mounting holes and center is 0.11265 m while for disc 2, it is 0.03799 m. The first set of balancing weights are $m_1 = 1.262$ g and $m_2 = 3.926$ g. The second set are $m_1 = 1.415$ g and $m_2 = 4.103$ g. We are going to identify the supporting stiffness and damping coefficients of the two magnetic bearings A and H.

The digital control system is based on the Innovative Integration M6713 PCI board and a TI C6713B 32-bit floating point digital signal processing (DSP) chip is used for the implementation of the digital control algorithm with an updating frequency around 12 kHz. Besides the DSP, a Labview data acquisition console is also added to interface with the computer for additional data logging. The data logging function is written in Labview 2010 and the sensor measurements and control outputs of all four control axes are saved at 6.4 KHz, which are much higher than the logging function provided by the DSP graphic user interface. They are also converted from time domain response to frequency domain response using the FFT block provided by Labview so it is possible to precisely identify at which frequency the maximum vibration happens. The rotating speed is also saved at 6.4 KHz, so these information can be used to identify the unbalance weight and estimate the stiffness and damping coefficients. Identification of AMB support parameters requires the steady state rotor displacement amplitude and phase information at AMB locations. The displacement amplitudes are obtained through eddy current sensors and the phase information is obtained through fiber optic sensors.

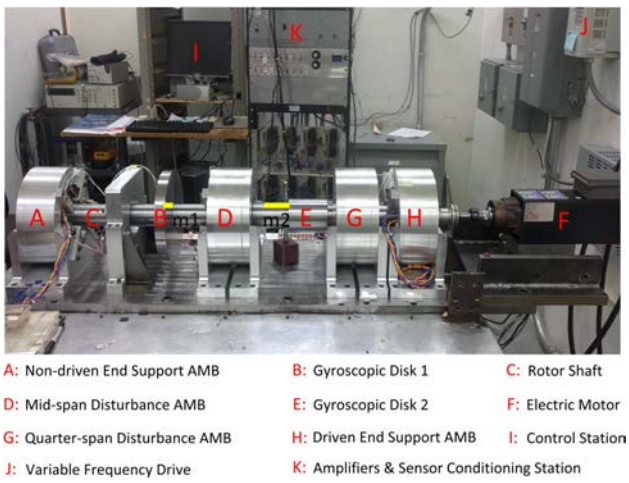

Figure 1: A Five DOF rotor AMB test rig with balancing weights m_1 and m_2.

B. Unbalance Response Based Identification

Shown in Fig. 2 is the schematic of the rotor AMB test rig we are to verify the unbalance response based identification method on.

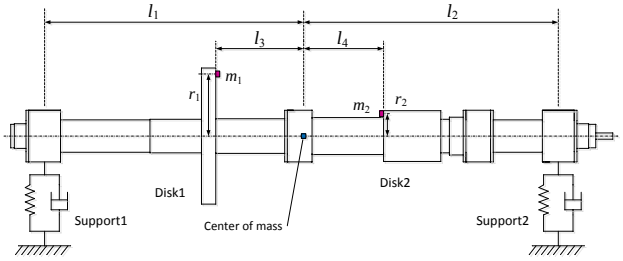

Figure 2: The schematic of the rotor AMB test rig.

In the Fig 2, l_1 and l_2 respectively represent the distances from the AMBs at both ends of the rotor to the rotor centroid, l_3 and l_4 are respectively the distances from disk 1 and disk 2 to the rotor centroid, m_1 and m_2 are the balancing weights attached respectively to the left and right disks, r_1 and r_2 are the distances between the disk centers and locations of the balancing weights.

We will model the AMBs with a combination of springs and dampers. The effects of unbalance force on the rotor center of mass and the effect of AMB force are equivalent to each other. The following equations are derived respectively from the balance of force and the balance of torque,

$$m\ddot{x}_c = f_{ux1} + f_{ux2} + f_{x1} + f_{x2}, \quad (1)$$
$$m\ddot{y}_c = f_{uy1} + f_{uy2} + f_{y1} + f_{y2}, \quad (2)$$
$$I_t\ddot{\theta}_y = -f_{ux1}l_3 + f_{ux2}l_4 - f_{x1}l_1 + f_{x2}l_2 - I_p\Omega\dot{\theta}_x, \quad (3)$$
$$I_t\ddot{\theta}_x = -f_{uy1}l_3 + f_{uy2}l_4 - f_{y1}l_1 + f_{y2}l_2 + I_p\Omega\dot{\theta}_y, \quad (4)$$

where x_c and y_c are the movements of the rotor center of mass in the x and y directions, respectively, m is the rotor mass, f_{ux1}, f_{ux2}, f_{uy1} and f_{uy2} are the unbalance forces generated by the balancing weights, f_{x1}, f_{x2}, f_{y1} and f_{y2} are the supporting forces from the AMBs, θ_x and θ_y are the rotor tilt angles in the x and y axes, I_t and I_p are respectively the transverse and polar moments of inertias, and Ω is the rotor rotating speed.

The AMB supporting forces can be expressed as

$$\begin{aligned} f_{x1} &= -\left(k_{x1}(\Omega)x_1 + c_{x1}(\Omega)\dot{x}_1\right), \\ f_{y1} &= -\left(k_{y1}(\Omega)y_1 + c_{y1}(\Omega)\dot{y}_1\right), \\ f_{x2} &= -\left(k_{x2}(\Omega)x_2 + c_{x2}(\Omega)\dot{x}_2\right), \\ f_{y2} &= -\left(k_{y2}(\Omega)y_2 + c_{y2}(\Omega)\dot{y}_2\right), \end{aligned}$$

where $k_{xi}(\Omega)$, $c_{xi}(\Omega)$, $k_{yi}(\Omega)$ and $c_{yi}(\Omega)$, $i = 1, 2$, are the stiffness and damping coefficients of AMBs in the x and y directions, with $i = 1$ denoting the AMB at the left end and $i = 2$ denoting the AMB at the right end. For notational brevity, in what follows we will often drop the dependence on Ω of these coefficients, and simply write k_{xi}, c_{xi}, k_{yi} and c_{yi}.

Based on Eqs. (1)-(4), the motion equation of the rotor can be further derived in the following complex form [16]

$$M\ddot{q} + (C + \Omega G)\dot{q} + Kq = F_0 e^{j\Omega t}, \quad (5)$$

where M is the rotor mass matrix, C is the support damping matrix, G is the gyroscopic effect matrix, K is the support stiffness matrix, $F_0 e^{j\Omega t}$ is the rotor unbalance force vector, and $q = q_0 e^{j\Omega t}$ are the rotor displacements vector with $q_0 = [x_1 \;\; x_2 \;\; y_1 \;\; y_2]^{\mathrm{T}}$. Matrices M, K, G and C are defined as follows,

$$M = \frac{1}{L}\begin{bmatrix} ml_2 & ml_1 & 0 & 0 \\ -I_t & I_t & 0 & 0 \\ 0 & 0 & ml_2 & ml_1 \\ 0 & 0 & -I_t & I_t \end{bmatrix},$$

$$K = \begin{bmatrix} k_{x1} & k_{x2} & 0 & 0 \\ -k_{x1}l_1 & k_{x2}l_2 & 0 & 0 \\ 0 & 0 & k_{y1} & k_{y2} \\ 0 & 0 & -k_{y1}l_1 & k_{y2}l_2 \end{bmatrix},$$

$$G = \frac{1}{L}\begin{bmatrix} 0 & 0 & 0 & 0 \\ 0 & 0 & -I_p & I_p \\ 0 & 0 & 0 & 0 \\ I_p & -I_p & 0 & 0 \end{bmatrix},$$

$$C = \begin{bmatrix} c_{x1} & c_{x2} & 0 & 0 \\ -c_{x1}l_1 & c_{x2}l_2 & 0 & 0 \\ 0 & 0 & c_{y1} & c_{y2} \\ 0 & 0 & -c_{y1}l_1 & c_{y2}l_2 \end{bmatrix},$$

where L is the rotor span.

The total unbalance excitation vector F_0 is given by

$$F_0 = \begin{bmatrix} f_1 + f_2 \\ -f_1l_3 + f_2l_4 \\ -j(f_1 + f_2) \\ -j(f_1l_3 - f_2l_4) \end{bmatrix}, \quad (6)$$

where

$$f_1 = m_1r_1\Omega^2 e^{-j\phi_1},$$
$$f_2 = m_2r_2\Omega^2 e^{-j\phi_2},$$

with ϕ_1 and ϕ_2 being the phase angles for the two balancing weights.

Substitution of $q = q_0 e^{j\Omega t}$ into (5) results in

$$j\Omega Cq_0 + Kq_0 = F_0 + (\Omega^2 M - j\Omega^2 G)q_0. \quad (7)$$

The values of the AMB support parameters can be solved from expanded Eq. (7), which can be reorganized into the following two equations,

$$Q_xP_x = F_x, \quad (8)$$
$$Q_yP_y = F_y, \quad (9)$$

where

$$Q_x = \begin{bmatrix} x_1 & x_2 \\ -l_1x_1 & l_2x_2 \end{bmatrix},$$

$$P_x = \begin{bmatrix} k_{x1} + j\Omega c_{x1} \\ k_{x2} + j\Omega c_{x2} \end{bmatrix},$$

$$Q_y = \begin{bmatrix} y_1 & y_2 \\ -l_1 y_1 & l_2 y_2 \end{bmatrix},$$

$$P_y = \begin{bmatrix} k_{y1} + j\Omega c_{y1} \\ k_{y2} + j\Omega c_{y2} \end{bmatrix},$$

$$F_x = \begin{bmatrix} f_1 + f_2 \\ -f_1 l_3 + f_2 l_4 \end{bmatrix} + \frac{\Omega^2}{L} \begin{bmatrix} ml_2 & ml_1 & 0 & 0 \\ -I_t & I_t & -jI_p & jI_p \end{bmatrix} \begin{bmatrix} x_1 \\ x_2 \\ y_1 \\ y_2 \end{bmatrix},$$

$$F_y = \begin{bmatrix} -j(f_1 + f_2) \\ -j(f_1 l_3 - f_2 l_4) \end{bmatrix} + \frac{\Omega^2}{L} \begin{bmatrix} 0 & 0 & ml_2 & ml_1 \\ jI_p & -jI_p & -I_t & I_t \end{bmatrix} \begin{bmatrix} x_1 \\ x_2 \\ y_1 \\ y_2 \end{bmatrix}.$$

Then we can solve P_x and P_y from Eqs. (8) and (9) to get the nominal values of the support parameters k_{xi}, c_{xi}, k_{yi} and c_{yi}, $i = 1, 2$,

$$P_x = Q_x^{-1} F_x, \quad P_y = Q_y^{-1} F_y.$$

We denote the nominal values as $k_{xi}^0(\Omega)$, $c_{xi}^0(\Omega)$, $k_{yi}^0(\Omega)$ and $c_{yi}^0(\Omega)$, $i = 1, 2$.

C. Parameter Rectification Based on Response Surface

In the unbalance response identification procedure described in the previous subsection, the rigid rotor model is adopted, which is expected to result in substantial identification errors. We will adopt the response surface approach to improve the precision. The response surface approach relies on the finite element model of the flexible rotor.

Because the coupling between the x and y axes of a radial AMB is small, we will establish an error response surface based on four support parameters in the x and y axes independently. Four control quadrants are assigned to each AMB and each control channel covers the two opposing quadrants. The top two quadrants both have 45° offset from the vertical so the two control channels can evenly carry the rotor weight, which makes the dynamics for both x and y axes almost identical. Therefore, the error response surfaces in the x and y axes can be established similarly. The error response surfaces in the x axes are formulated as follows,

$$\begin{aligned} \Delta k_{x1} &= F_1(k_{x1}^0, k_{x2}^0, c_{x1}^0, c_{x2}^0), \\ \Delta k_{x2} &= F_2(k_{x1}^0, k_{x2}^0, c_{x1}^0, c_{x2}^0), \\ \Delta c_{x1} &= F_3(k_{x1}^0, k_{x2}^0, c_{x1}^0, c_{x2}^0), \\ \Delta c_{x2} &= F_4(k_{x1}^0, k_{x2}^0, c_{x1}^0, c_{x2}^0), \end{aligned}$$

where $F_i(k_{x1}^0, k_{x2}^0, c_{x1}^0, c_{x2}^0)$, $i = 1, 2, 3, 4$, are polynomials in terms of the four nominal AMB support parameters k_{x1}^0, k_{x2}^0, c_{x1}^0 and c_{x2}^0, as identified by the unbalance response method from the experimental measurements.

We approximate these error response surfaces with polynomials of fifth degree in the normalized nominal stiffness and damping coefficients $\tilde{k}_{x1}$, $\tilde{k}_{x2}$, $\tilde{c}_{x1}$, $\tilde{c}_{x2}$. Take Δk_{x1} at speed Ω as an example, we have

$$\begin{aligned} \Delta k_{x1} = {} & \beta_0(\Omega) + \beta_1(\Omega)\tilde{k}_{x1} + \beta_2(\Omega)\tilde{k}_{x2} + \beta_3(\Omega)\tilde{c}_{x1} \\ & + \beta_4(\Omega)\tilde{c}_{x2} + \cdots + \beta_{17}(\Omega)(\tilde{k}_{x1})^5 + \beta_{18}(\Omega)(\tilde{k}_{x2})^5 \\ & + \beta_{19}(\Omega)(\tilde{c}_{x1})^5 + \beta_{20}(\Omega)(\tilde{c}_{x2})^5 + \beta_{21}(\Omega)\tilde{k}_{x1}\tilde{k}_{x2} \\ & + \beta_{22}(\Omega)\tilde{k}_{x1}\tilde{c}_{x1} + \cdots + \beta_{26}(\Omega)\tilde{c}_{x1}\tilde{c}_{x2}. \end{aligned}$$

The procedure for determining the coefficients $\beta_i(\Omega)$, $i = 0, 1, \cdots, 26$, is described in detail in [16] and is briefly summarized in Fig. 3.

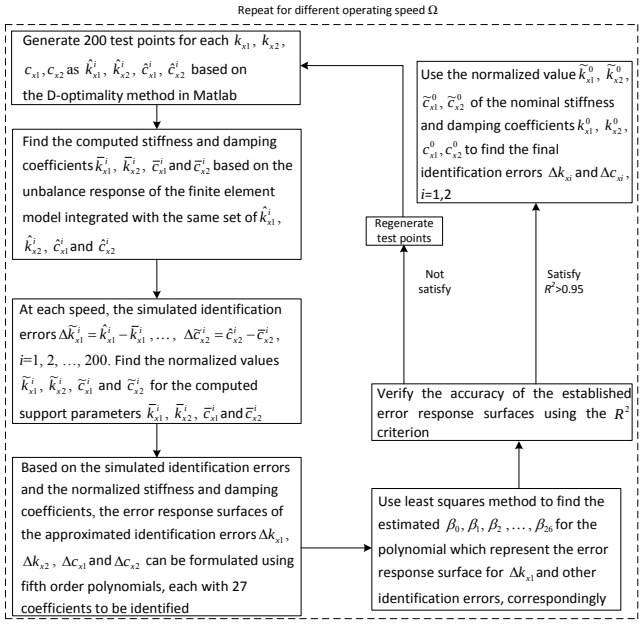

Figure 3: The procedure for determining the coefficients of the error response surfaces.

With these coefficients determined, the identification error can be calculated as

$$\begin{aligned} \Delta k_{x1}(\Omega) = {} & \beta_0(\Omega) + \beta_1(\Omega)\tilde{k}_{x1}^0(\Omega) + \beta_2(\Omega)\tilde{k}_{x2}^0(\Omega) \\ & + \beta_3(\Omega)\tilde{c}_{x1}^0(\Omega) + \beta_4(\Omega)\tilde{c}_{x2}^0(\Omega) + \cdots \\ & + \beta_{17}(\Omega)(\tilde{k}_{x1}^0(\Omega))^5 + \beta_{18}(\Omega)(\tilde{k}_{x2}^0(\Omega))^5 \\ & + \beta_{19}(\Omega)(\tilde{c}_{x1}^0(\Omega))^5 + \beta_{20}(\Omega)(\tilde{c}_{x2}^0(\Omega))^5 \\ & + \beta_{21}(\Omega)\tilde{k}_{x1}^0(\Omega)\tilde{k}_{x2}^0(\Omega) + \cdots \\ & + \beta_{26}(\Omega)\tilde{c}_{x1}^0(\Omega)\tilde{c}_{x2}^0(\Omega), \end{aligned}$$

where $\tilde{k}_{x1}^0(\Omega)$, $\tilde{k}_{x2}^0(\Omega)$, $\tilde{c}_{x1}^0(\Omega)$, $\tilde{c}_{x2}^0(\Omega)$ are normalized values of $k_{x1}^0(\Omega)$, $k_{x2}^0(\Omega)$, $c_{x1}^0(\Omega)$ and $c_{x2}^0(\Omega)$.

The other error response surfaces on the x axis, $\Delta k_{x2}(\Omega)$, $\Delta c_{x1}(\Omega)$ and $\Delta c_{x2}(\Omega)$, can be formulated and obtained in the same procedure.

The final identified AMB stiffness and damping coefficients on the x axis can be obtained as,

$$k_{x1}(\Omega) = k_{x1}^0(\Omega) + \Delta k_{x1}(\Omega),$$

$$k_{x2}(\Omega) = k^0_{x2}(\Omega) + \Delta k_{x2}(\Omega),$$
$$c_{x1}(\Omega) = c^0_{x1}(\Omega) + \Delta c_{x1}(\Omega),$$
$$c_{x2}(\Omega) = c^0_{x2}(\Omega) + \Delta c_{x2}(\Omega).$$

III. Experimental Verification

The experimental identification process for the stiffness and damping coefficients is summarized in Fig. 4.

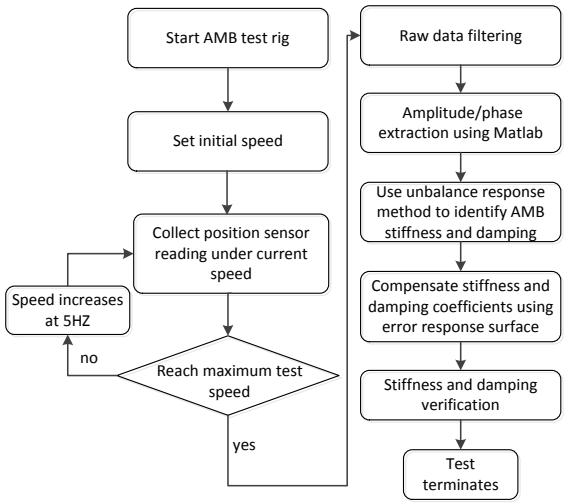

Figure 4: Experimental identification process.

A. Identification Results

The data logging starts from 600 rpm to 6000 rpm. The rotor displacements and rotating speed are saved every 300 rpm for around 10 seconds. The measured displacements go through unbalance signal filtering using Kaiser bandpass filters and zero phase digital filters to extract the steady state amplitude and phase information. Based on the experimental measurements, the nominal values of the stiffness and damping coefficients can be identified using the unbalance response method described in Subsection II-B.

To construct the error response surfaces as described in Subsection II-C, we create a finite element model of the test rig in MSC.Patran. The stiffness and damping coefficients of AMBs are closely related to the feedback control gains. Generally, the control gains for each control channel are slightly different, so the stiffness and damping coefficients for each axis are different. Therefore, we used different test points in constructing the error response surfaces for the support parameters. Two virtual balancing weights are attached to the model discs and then we analyze the unbalance response through the finite element model from 600 rpm to 6000 rpm with an interval of 300 rpm. Based on the rectification method proposed in Subsection II-C, we can develop the error response surfaces for different operating speeds.

The identified stiffness and damping coefficients for the two sets of balancing weights are shown in Figs. 5 and 6. It is observed that the AMB stiffness coefficients on both axes increase with the operating speed because the frequency of the unbalance force is directly related to the operating speed.

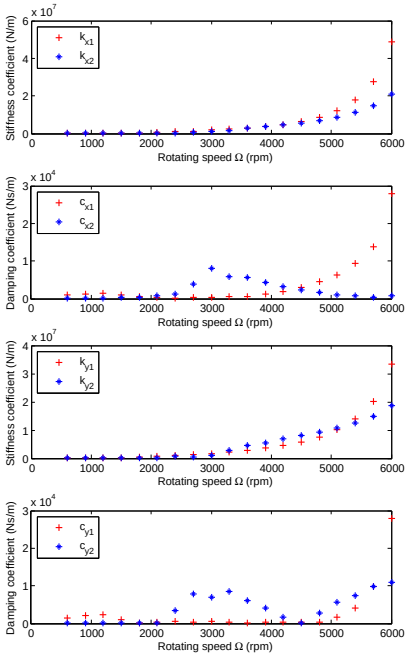

Figure 5: Identified stiffness and damping coefficients for Set 1 of balancing weights. The upper two plots: k_x and c_x; The lower two plots: k_y and c_y.

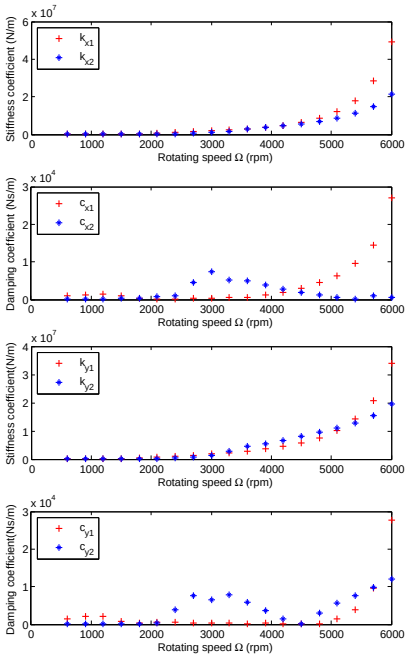

Figure 6: Identified stiffness and damping coefficients for Set 2 of balancing weights. The upper two plots: k_x and c_x; The lower two plots: k_y and c_y.

B. Verification of the Identification Results

To verify the accuracy of the identification results, we integrate identified stiffness and damping coefficients with the finite element model of the rotor to form a full model of the rotor-AMB test rig. Based on this model, we obtain the model unbalance response and compare them with the experimental

measurements. The comparison results are shown in Figs. 7 and 8.

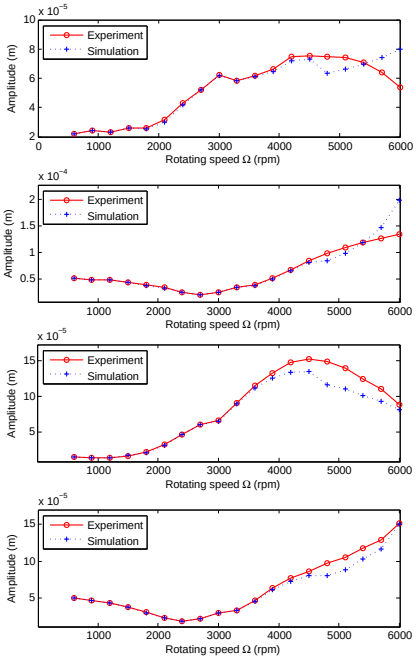

Figure 7: Comparison of displacements between experiments and simulation under Set 1 of balancing weights. The upper two plots: x_1 and x_2; The lower two plots: y_1 and y_2.

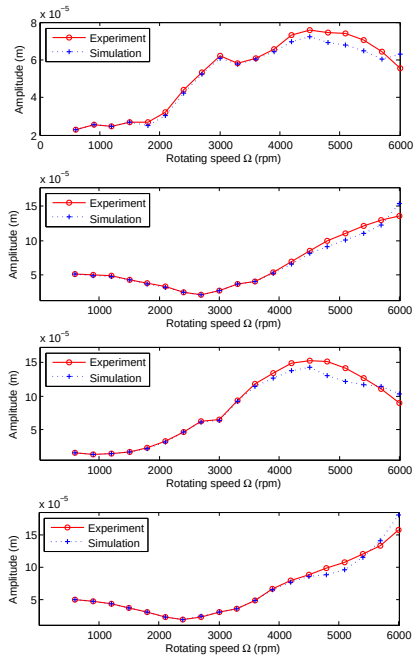

Figure 8: Comparison of displacements between experiments and simulation under Set 2 of balancing weights. The upper two plots: x_1 and x_2; The lower two plots: y_1 and y_2.

It can be observed that the unbalance response from the finite element model closely agrees with the experimental measurements at speeds ranging from 600 rpm to 6000 rpm. This verifies the effectiveness of the identification method.

IV. Conclusions

This paper presented the experimental verification of an unbalance response based identification method we recently proposed to identify AMB stiffness and damping coefficients. Considering the rotor flexibility, the final AMB support parameters are determined as the sum of the nominal values calculated from the experimental unbalance response of a flexible rotor AMB test rig and the identification errors derived from the error response surfaces. The identified support parameters are combined with the finite element model of the test rig to generate unbalance response and they are compared with experimental measurements. Their close agreements indicate that the proposed method is effective in identifying the AMB stiffness and damping coefficients.

V. Acknowledgements

This work was in part supported by National Natural Science Foundation of China (No. 51075200) and the Jiangsu provincial Natural Science Foundation (No. BK2011070).

References

[1] G. Schweitzer and E. H. Maslen, *Magnetic Bearings*. Springer, 2009.

[2] R. Humphris, R. D. Kelm, and D. W. Lewis, "Effect of control algorithms on magnetic journal bearing properties," *Journal of Engineering for Gas Turbines and Power, Transactions of the ASME*, vol. 108, pp. 624–632, 1986.

[3] L. Yu, *Controllable Magnetic Levitationrotor System*. Beijing: Science Press, 2003.

[4] Y. Hu, Z. Zhou, and Z. Jiang, *Foundation Theory and Application of Active Magnetic Bearing*. Beijing: China Machine Press, 2006.

[5] H. Wang and Z. Jiang, "Research on the electromagnetic force and the stiffness of the active magnetic bearing," *Journal of Tianjin University*, vol. 10(4), pp. 15–20, 1992.

[6] X. Wang, "Parametric Design and Application Investigation of Electromagnetic Bearing System," Ph.D. Dissertation, Xi'an Jiaotong University, Xi'an, 1994.

[7] G. Schweitzer, R. Siegwart, and R. Herzog., "Stiffness of magnetic bearings," in *Proc. of 4th Int. Symposium on Magnetic Bearings*, Switzerland, 1994, pp. 251–256.

[8] Z. Yang, L. Zhao, and H. Zhao, "Automatic measurement of dynamic stiffness for active magnetic bearings," *Chinese Journal of Mechanical Engineering*, vol. 37(3), pp. 25–29, 2001.

[9] H. Wu, "Study on dynamic characteristics for AMB suspension rotor," Ph.D. Dissertation, Wuhan University of Techonology, Wuhan, 2005.

[10] X. Wang and C. Gao, "Measurement methodof stiffnessfor magnetic bearings," *China Mechanical Engineering*, vol. 21(8), pp. 889–891, 2010.

[11] J. Zhou and J. Lin, "The theoretical analysis and experimental research on the supporting characteristics in axial magnetic bearing," *Machine Design and Research*, vol. 26(5), pp. 71–73, 2010.

[12] Y. Shen and L. Yu, "Identification of dynamic coefficients of active magnetic bearings," *Machine Tool and Hydraulics*, vol. 6, pp. 8–11, 2001.

[13] O. D. Santiago and L. S. Andres, "Field methods for identification of bearing support parameters-part i: Identification from transient rotor dynamic response due to impacts," *Journal of Engineering for Gas Turbines and Power*, vol. 129, pp. 205–212, 2007.

[14] Z. Li, J. Zhang, and C. Lu, "Study on identification of dynamic characteristics of flexible rotor system from the rotor's disequilibrium response," *Lubrication Engineering*, vol. 5, pp. 23–25, 1999.

[15] O. D. Santiago and L. S. Andres, "Field methods for identification of bearing support parameters-part ii: Identification from rotor dynamic response due to imbalances," *Journal of Engineering for Gas Turbines and Power*, vol. 129, pp. 213–219, 2007.

[16] J. Zhou, L. Di, C. Chen, Y. Xu, and Z. Lin, "A rotor unbalance response based approach to the identification of the stiffness and damping coefficients of active magnetic bearings," submitted for publication.